CATASTROPHIC RUPTURE OF LUNAR ROCKS: A MONTE CARLO SIMULATION

F. HÖRZ

Geology and Geophysics Branch, NASA Johnson Space Center, Houston, Tex., U.S.A.

E. SCHNEIDER*

The Lunar Science Institute, Houston, Tex., U.S.A.

D. E. GAULT

Planetary Science and Applications Branch, Space Science Division, NASA Ames Research Center, Moffett Field, Calif., U.S.A.

J. B. HARTUNG

Dept. of Earth and Space Sciences, State University of New York, Stony Brook, N.Y., U.S.A.

and

D. E. BROWNLEE

Dept. of Astronomy, University of Washington, Seattle, Wash., U.S.A.

Abstract. A computer model based on Monte Carlo techniques was developed to simulate the destruction of lunar rocks by 'catastrophic rupture' due to meteoroid impact. Energies necessary to accomplish catastrophic rupture were derived from laboratory experiments. A crater-production rate derived from lunar rocks was utilized to calculate absolute time scales.

Calculated median survival times for crystalline lunar rocks are 1.9, 4.6, 10.3, and 22 m.y. for rock masses of 10, 10^2, 10^3, and 10^4 g respectively. Corresponding times of 6, 14.5, 32, and 68×10^6 yr are required, before the probability of destruction reaches 0.99. These results are consistent with absolute exposure ages measured on returned rocks.

Some results also substantiate previous conclusions reached by others: the catastrophic rupture process is significantly more effective in obliterating lunar rocks compared to mass wasting by single particle abrasion. The view is also corroborated that most rocks presently on the lunar surface are either exhumed from the regolith or fragments of much larger boulders, rather than primary ejecta excavated from pristine bedrock.

1. Introduction

Photogeological studies and analyses of returned lunar materials present overwhelming evidence that the lunar regolith is a clastic sediment caused by meteorite impact comminution processes. Not only is the meteoroid bombardment responsible for excavating materials from pristine bedrock, but the freshly generated ejecta are also subject to repetitive bombardment with the net effect that rocks are continuously eroded and ruptured. Mechanisms other than meteoroid impact seem to be of little significance, if at all, for the destruction of hand specimen size rocks (Ashworth and McDonnell, 1973).

The destruction of rocks by meteoroid bombardment is accomplished via two different mechanisms: 'single particle abrasion' and 'catastrophic rupture' (Gault,

* Permanent address: Max-Planck-Institut für Kernphysik, 6900 Heidelberg, F.R.G.

The Moon **13** (1975) 235–258.

1969; Shoemaker, 1971; Gault *et al.*, 1972; Ashworth and McDonell, 1973; Hörz *et al.*, 1974). Single particle abrasion is caused by relatively small cratering events that result in an effect similar to sandblasting. This gradual 'mass wasting' (Crozaz *et al.*, 1971) leads to rounding and a marked decrease of angularity of lunar rocks. 'Catastrophic rupture' refers to the fragmentation of a rock due to one or more direct hits of any meteorite(s) energetic enough to break apart an entire rock specimen (Figure

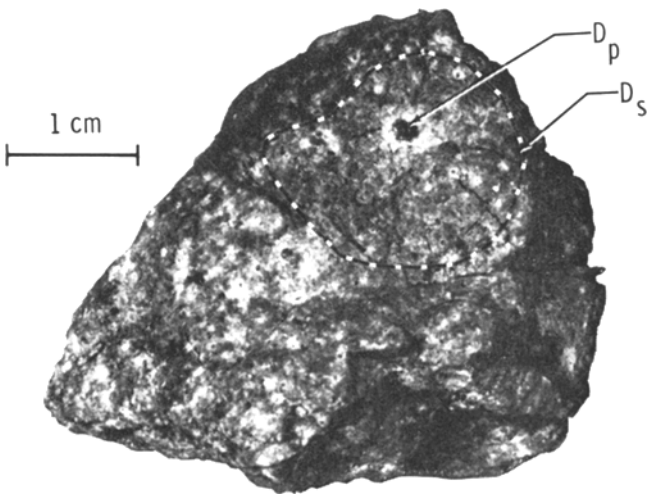

Fig. 1. Example of the catastrophic rupture process (rock 73155). Note the prominent fracture system emanating from a microcrater of approximately 3 mm pit diameter (D_p). A slightly more energetic event would have lead to catastrophic rupture. The corresponding spall zone (D_s) is also indicated; note that its diameter is significantly less than the diameter of the rock.

1). Both the single particle abrasion as well as the catastrophic rupture process have been treated previously. The results of these calculations are summarized in Table I.

According to Table I the single particle abrasion or mass wasting process removes in the order of 1 mm/10^6 yr of rock surface for rocks in the 1 kg mass range. These calculated results are in good agreement with erosion rates directly measured via solar flare and galactic particle track gradients in lunar rocks as well as depth profiles of shortlived radio isotopes, e.g., ^{26}Al or ^{53}Mn, as summarized recently by Crozaz *et al.* (1974).

Calculated mean surface residence times of lunar rocks, however, vary greatly in previous analyses (see Table I). The differences are due to various assumptions concerning both the flux of meteorites and/or to the amount of energy necessary to rupture any given rock mass. Though some of the discrepancies will be discussed below, the mean residence times listed in Table I suffer from a basic shortcoming in that they are analytically derived averages.

Because the random nature of meteoroid impact in both space and time results in unique bombardment histories for any finite, small surface area, a variety of probabil-

TABLE I

Single particle abrasion rates and mean surface residence times of Lunar rocks according to previous calculations

Single particle abrasion (mm 10^6 yr^{-1})		
Shoemaker (1971)[a]	1.4 –2.1	(on 1–10 cm diam. rocks)
Shoemaker (1971)[b]	0.041–0.062	(on 1–10 cm diam. rocks)
Gault *et al.* (1972)	1.8	(on 10 cm diam. rock)
Gault *et al.* (1972)	2.0	(on 100 cm diam. rock)
Ashworth and McDonnell (1973)	0.1 –0.01	(on 10 cm diam. rock)
Neukum (1973)	1.0	(unspecified dimension)
Hörz *et al.* (1974)	0.4 –0.6	(on 6 cm diam. rock)
Mean surface residence time		
Shoemaker (1971)[a]	4×10^6 yr	(3–6 cm diam. rocks)
Shoemaker (1971)[b]	17×10^6 yr	(3–6 cm diam. rocks)
Gault *et al.* (1972)	0.1×10^8 yr	(1 cm diam. rock)
	2×10^6 yr	(10 cm diam. rock)
	60×10^6 yr	(100 cm diam. rock)
Ashworth and McDonnell (1973)[c]	600×10^6 yr	(10 cm diam. rock)
	3300×10^6 yr	(10 m diam. rock)

[a] Constant flux over the entire mare history, i.e., approximately 3.7×10^9 yr.
[b] Best estimate for the recent erosion rate, i.e., the last few 10^6 yr
[c] Combined effects of solar wind sputtering, single particle abrasion and catastrophic rupture.

istic models or Monte Carlo studies have been advanced recently to gain a more quantitative insight into certain impact related regolith processes such as overall growth of regolith (Quaide and Oberbeck, 1975), the mixing and turnover of regolith (Gault *et al.*, 1974; Arnold, 1975), the development of microcrater populations (Hartung *et al.*, 1973) and the single particle abrasion (Hörz *et al.*, 1974). These models illustrated that the description of an 'average' condition is in most cases not adequate for interpretation of specific lunar samples, because each sample has a unique history that may significantly deviate from the average condition. Deviation from the average is of particular importance for the interpretation of rock exposure histories because only such rocks which actually survived the catastrophic rupture process could have been collected; thus only 'survivors' are available for analysis and they cannot reflect a true average condition.

Therefore, a computer model utilizing Monte Carlo (MC) techniques was developed to simulate random impact in space and time. The basic input data reflect our most recent understanding of the micrometeoroid flux and appropriate impact cratering mechanics, in particular, a better understanding of the rupture process. The objectives of this model are to gain some insight into the statistics of the destruction process and the potential surface histories of lunar rocks as an aid for the interpretation of measured, absolute surface residence times and resulting regolith dynamics.

2. The Monte Carlo Model

A. RUPTURE ENERGY

Gault and Wedekind (1969) presented impact cratering experiments that assessed a projectile's total kinetic energy causing catastrophic rupture of glass-spheres ranging in size from 4.5 to 10 cm diam. One of us (DEG) has subsequently carried out similar experiments on basalt and granite spheres and/or cubes as well as bonded sand targets to simulate various target strengths. 'Rupture' was accomplished by definition when the largest fragment remaining constituted $\leqslant 50\%$ of the original target mass. The following relationship was obtained (see also Gault *et al.*, 1972)

$$E_{R_g} = 4.6 \times 10^6 \, S_c^{0.45} r^{-0.225}, \tag{1}$$

where E_{R_g} is the critical rupture energy per gram target material (in ergs), S_c is the unconfined compressive strength of the target (in kb) and r is the radius of a spherical target (in cm). For crystalline rocks of 3 kb compressive strength, the above expression can be rewritten to yield the critical energy (E_R) required to rupture any given mass (m) as

$$E_R = 7.5 \times 10^6 \times r^{-0.225} \times m = 8.4 \times 10^6 \times \delta^{0.075} \times m^{0.925}. \tag{2}$$

It is important to note that E_R does not represent the total energy actually expended during the rupture process. Instead it represents the minimum kinetic energy of a projectile that upon impact releases sufficient energy to accomplish rupture of a given rock mass.

Furthermore, Gault (1973) presents the following relationship between projectile kinetic energy (E_{kin}) and resulting crater diameter (D_s) as

$$D_s = 10^{-2.823} \delta_p^{1/6} \delta_t^{-1/2} E_{\text{kin}}^{0.370}, \tag{3}$$

where δ_p and δ_t are projectile and target density respectively (g cm^{-3}). Thus it is possible to define the kinetic energy required to produce any crater diameter (Equation (3)) and to rupture any given rock mass (Equation (2)).

These relationships are illustrated in Figure 2, assuming for both target and projectile a density of 3 g cm^{-3}. The empirically derived data utilized in this report relating critical crater diameter (D_{sc}), projectile energy, and rock mass destroyed are annotated (Gault *et al.*, 1972). Any crater $\geqslant D_{sc}$ will rupture an associated rock mass. Taking a typical ratio of 4:1 for the diameter of the spall-zone (D_s) and central glass lined pit (D_p) for lunar microcraters, where a spall zone is often not observable, (Schneider and Hörz, 1974), a critical pit diameter ($D_{pc} = \frac{1}{4} D_{sc}$) may be derived that should have lead to catastrophic rupture and that therefore should not be observable on returned lunar rocks. To test the validity of these relationships, *maximum* pit diameters observed (D_{po}) on a variety of lunar rocks of mass 'x' are plotted as a function of rock mass. Extensive fracture systems indicative of incipient rupture were observed around a few pits. All pit diameters observed are less than those calculated and thus are consistent with the established relationship of critical rupture energy and

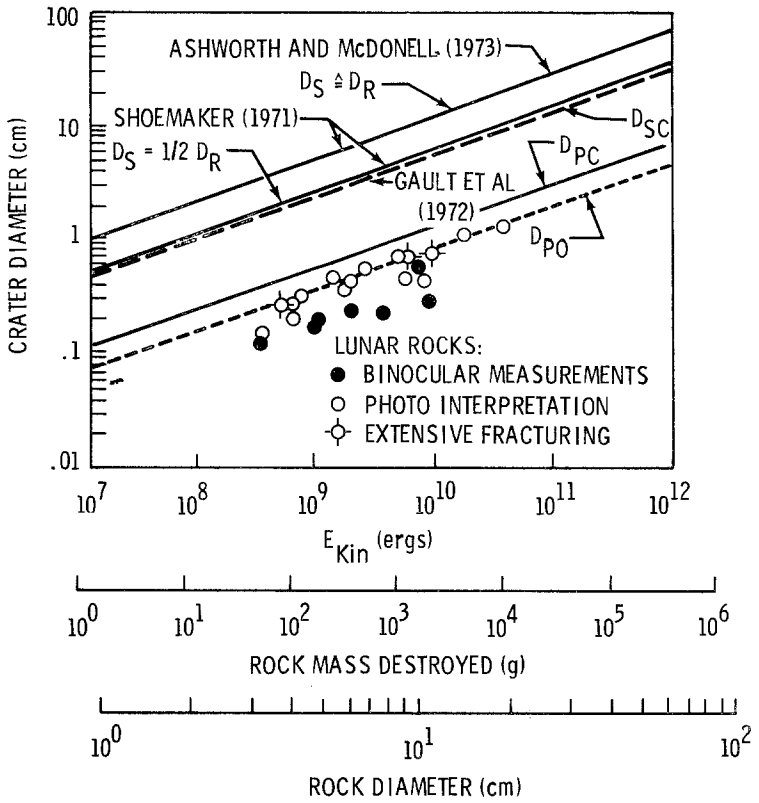

Fig. 2. Graphical display of Equation (2) and (3) illustrating the rupture criteria employed in this model (labeled Gault *et al.*, 1972) and the criteria used by others in comparison to crater measurements on lunar rocks.

crater diameter. For additional comparison the rupture criteria utilized by Shoemaker (1971) and Ashworth and McDonnell (1973) are illustrated. They consider a rock destroyed if it experiences an impact event that has a diameter (D_s) larger than the diameter of the rock (D_R), i.e., $D_s \geqslant E_R$. These are unrealistically high values and are in disagreement with the above cratering experiments as well as analyses of lunar rocks (see Figure 1 and 2). Shoemaker (1971) proposed a second relationship for rupture where $D_s = \frac{1}{2}D_R$; this relationship is close to the value employed in the analysis below.

According to Gault and Wedekind (1969) and additional unpublished data (DEG) the rupture energy may be delivered not only by a single event of $\geqslant E_R$, but also by a variety of smaller events that have an equivalent total energy. Firm experimental data exist only for cases where 2 events, each of $\frac{1}{2}E_R$, have lead to catastrophic rupture of the target. Observations on lunar rocks (Figure 2) indicate that fracture systems develop at pit diameters of approximately $\frac{1}{2}$ the diameter of the predicted value, corresponding to events that have approximately $\frac{1}{10}E_R$. Thus we consider all impact events with energies $\geqslant 0.1E_R$ to be effective in contributing to catastrophic rupture;

this will lead to significant differences with the models of Shoemaker (1971) and Ashworth and McDonnell (1973).

B. PROJECTILE ENERGY DISTRIBUTION

According to Equation (3) any given crater diameter may be converted into the corresponding kinetic energy of the impacting particle. Consequently any measured crater size frequency distribution can be directly transformed into an energy frequency distribution without model dependent assumptions concerning meteoroid velocity and mass. Lunar microcraters ranging in size from $\approx 200\ \mu$m to ≈ 1 cm diam (D_s) have been measured by numerous workers (e.g., Hartung *et al.*, 1972; Morrison *et al.*, 1972; Neukum *et al.*, 1973). Production size frequency distribution for such craters is given by

$$N_c = KD_s^{-2.96}, \tag{4}$$

where N_c is the cumulative number of craters per unit area and K is a constant relating to exposure time. An identical distribution function was assumed for craters between 1 and 50 cm diam. Such an extrapolation to large craters is reasonable on the basis of measured energy frequency distributions of present-day meteoroid impacts (Latham *et al.*, 1973) and present-day mass distributions of interplanetary solid matter (Dohnanyi, 1972).

The cumulative crater frequency distribution represented by Equation (4) was converted into a cumulative energy distribution i.e., (4) in (3)

$$N_c = K(10^{-2.823}\delta_p^{1/6}\delta_t^{-1/2}E_{\text{kin}}^{0.370})^{-2.96} \tag{5}$$

$$= CE_{\text{kin}}^{-1.095}. \tag{6}$$

The above energy distribution function was used to graphically extrapolate the differential frequency of occurrence of arbitrary cratering energies with energy intervals differing in steps of $\frac{1}{10}E_{\text{kin}}$. This yielded the frequency of occurrence of cratering events ranging in energy from 0.1, 0.2, ..., $0.9E_R$. Events with energies $\geqslant 1.0E_R$ were not differentiated in detail; instead their cumulative number represented the energy class $\geqslant 1.0E_R$. The numerical results representing the probability of occurrence of any specific event are listed in Table II. Because the exponent in Equation (6) was taken to be constant for all energies considered, the probabilities listed in Table II may be used for any arbitrary energy and thus crater size interval operating on any arbitrary rock mass. As a consequence all results presented below are derived from *one* computer run only. All relative and absolute parameters discussed for various rock masses are derived analytically as will be described.

According to Figure 2, events as large as $10.0E_R$ are not expected to contribute to the destruction of a neighboring rock because the crater diameter (D_s) equals the rock diameter (D_R). Destruction of 2 closely spaced rocks due to a single impact event is possible at $\approx 50E_R$, depending on the precise location ($D_s \approx 1.65D_R$) and should occur at events $\geqslant 100E_R$, where $D_s \geqslant 2D_R$. It is not known whether these strictly

TABLE II

Basic input data into the computer model concerning probability of occurrence of specific cratering events

Fraction of total rupture energy	Probability of occurrence
0.1	0.00000–0.5270
0.2	0.5270 –0.7000
0.3	0.7000 –0.7817
0.4	0.7817 –0.8289
0.5	0.8289 –0.8596
0.6	0.8596 –0.8815
0.7	0.8815 –0.8980
0.8	0.8980 –0.9101
0.9	0.9101 –0.9200
$\geqslant 1.0$	0.9200 –1.0002

geometric considerations apply in reality because it is conceivable that an event of $D_s = 2D_R$ may not affect at all a neighboring rock. However, if $D_s \gg D_R$, destruction of multiple rocks must occur. The probabilities of occurrence of events $\geqslant 10.0E_R$ and $\geqslant 100E_R$ are 0.004 and 0.0005 respectively, according to Equation (6). Thus because of the extremely low probability of occurrence of events that may destroy multiple rocks, if at all, such events were not considered in this report and it is suggested that they will not significantly modify the results.

C. TEST SURFACE AND COMPUTER RUN

A computer test surface was divided into a grid system of 120×120 square cells resulting in 14400 impact centers simulating 14400 identical 'rocks' with a square cross section of unspecified absolute dimension. Random number generators determined impact coordinates and impact energies in accordance with the probabilities listed in Table II. Impact coordinates and the energy delivered by each event were recorded and continuously monitored per each cell in a cumulative fashion until the critical rupture energy had accumulated. 'Rock' (x_i/y_j) was then declared ruptured and removed from the existing rock inventory. Detailed bombardment histories were monitored only for such locations, i.e., 'rocks' that had experienced $\leqslant 1.0E_R$. However, all 14400 locations operated throughout the entire run as absolutely equivalent impact sites, regardless whether a site was or was not occupied by a rock.

The MC program therefore simulated a surface which was initially covered 100% with rocks of identical size. Cratering events occurred at the same rates on rocks and in interrock areas. Due to the random impact environment, the model will thus be valid also for situations, where only a fraction of the initial surface is covered by rocks, as long as such a fraction is statistically significant; whether this fraction is distributed evenly or scattered at random is not an important factor. Furthermore the square cross-section of our arbitrary rock population can be substituted by any other ge-

ometry; the model will be valid for any case as long as the absolute surface area occupied by rocks can be determined to be a statistically significant fraction of a reference surface.

3. Model Results

The actual computer results will be presented in this chapter and will be discussed in relative terms only, because standardized conditions were applied that are of general validity.

Figure 3 illustrates the destruction of rocks as a function of destruction time, with 'time' being linearly related to absolute number of craters produced. Both the cumulative and differential number of destroyed rocks are indicated. Any MC model will differ from general probability theory in a subtle way because (1) it employs a finite number of rocks and (2) it uses a particular set of random numbers. Thus MC modeling is effectively approximating general Poisson probabilities. Because of sufficient numbers of rocks, this approximation should be excellent in our case; however, data obtained for the last few surviving rocks are limited for general application. As a consequence the 100% destruction time in Figure 1 is defined as the period necessary to destroy 99.5% of the original rock population; the last remaining 0.5% may not be simulated with confidence using MC-techniques.

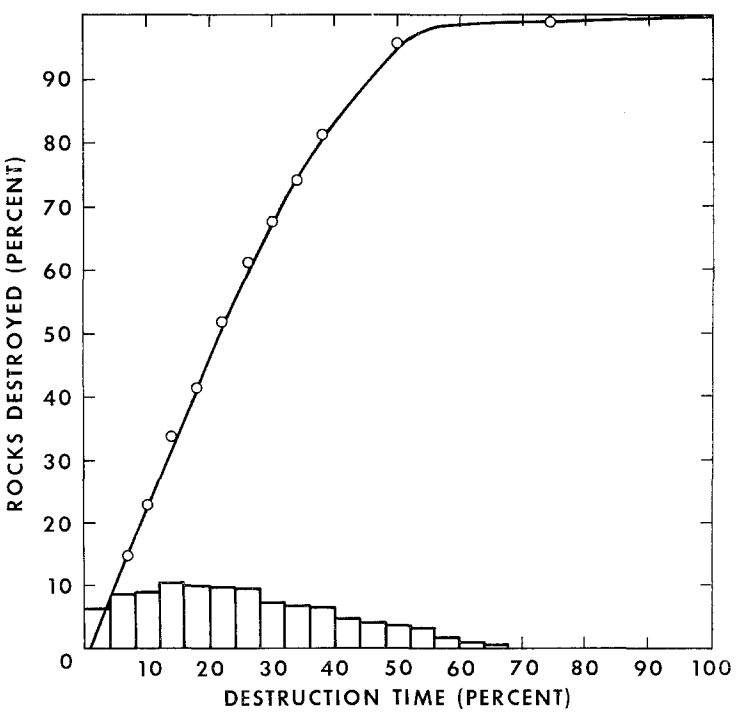

Fig. 3. Cumulative and differential number of rocks destroyed as a function of time ('100%' of time refers to the destruction of only 99.5% rocks; it is linearly related to the number of craters produced, which are not indicated).

Returning to the cumulative curve in Figure 3 it may be seen that 50% of all rocks are destroyed in 22% of the total time. Thus the 'median survival time' is approximately 5 times shorter than the time required to effectively destroy the original population. The differential histogram shows that the destruction process is of intermediate efficiency in the early stages, passes through a maximum centered around the median survival time and then declines asymptotically with increasing time. An explanation follows later.

Another prime result is illustrated in Figure 4 and concerns the fraction of the total available impact energy (E_0) for the entire reference surface (F_0) that has effectively

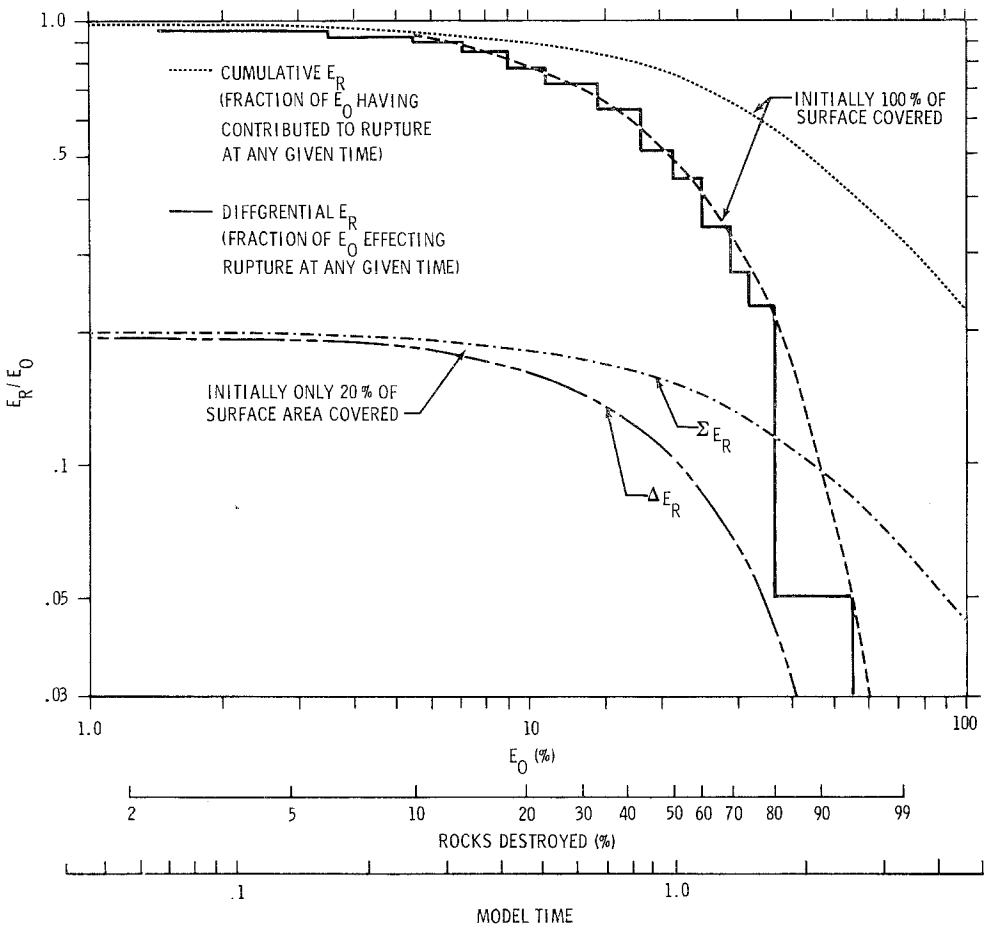

Fig. 4. Ratio of total available energy (E_0) and the fraction (E_R) actually contributing to the rupture process. These data were directly obtained from the computer run by monitoring the total number and energy magnitudes of all craters occurring (1) on the entire test surface (E_0) and (2) on the undestroyed 'cells' only (E_R). These data are plotted cumulatively and differentially; 100% E_0 is defined as the total influx to destroy 99.5% of the rocks. The 'rocks destroyed' and 'model time' are transferred from Figure 3, with unit time now being defined as the median survival time (=50% rocks destroyed).

contributed to the rupture of rocks (E_R). Because with increasing time more and more rocks are destroyed, a larger and larger fraction of the total energy will be wasted in between rocks. Referring to the cumulative curve in Figure 4 (100% case) it can be seen that only about 0.22 of the total impact energy has effectively contributed to the rupture of 99.5% rocks. Already at the median survival time (= 50% rocks destroyed) approximately 20% of the available energy was wasted. Considering the differential curve, the energy actually contributing to rupture at any particular time is of course a function of the fractional surface area (F_x) covered by rocks, i.e., $F_x/F_0 = E_R/E_0$. If initially only a fraction of the surface were covered with rocks (F_x'), the initial fraction of rupture energy would then be $E_R = (F_x' \cdot E_0)/F_0$. An example where $F_x' = 20\%$ is illustrated. As a consequence as long as a statistically significant fraction of the surface is covered by rock-specimen, it will take the same amount of absolute energy (E_0) and therefore the same amount of time to effectively destroy such a rock population.

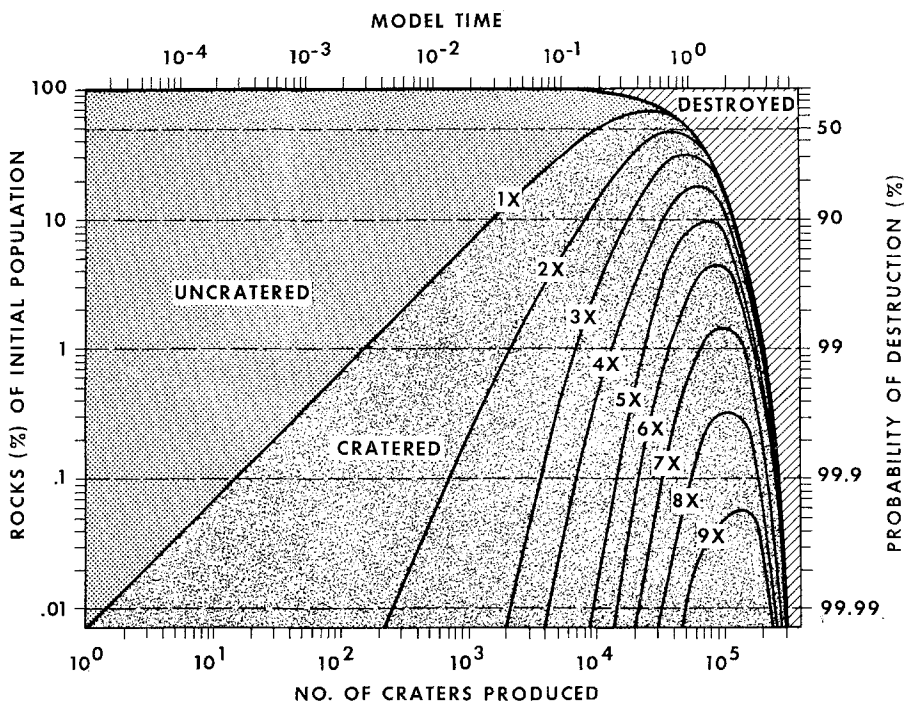

Fig. 5. Detailed bombardment history of the entire rock population. Number of craters produced and model time are linearly related, with unit time again being defined as median survival time. All percentages given are cumulative; differential percentages must be extrapolated in the following way: always put a vertical line through the plott, i.e., extract the status of the rock population per any given time. e.g., at model time 10^{-1} ($=5.5 \times 10^8$ craters) there are $\approx 0.15\%$ rocks impacted at least $4\times$ (a); 0.47% are impacted at least $3\times$ (b); 4.6% are impacted at least $2\times$ (c); 30% are impacted at least $1\times$ (d); 99% of the rocks survived (e); 1% was ruptured (f). Differential percentages are 0.15% of the rocks cratered at least $4\times$; 0.455% are cratered $3\times$ (a–b); 4.13% are cratered $2\times$ (c–b); 25.8% are impacted $1\times$ (d–c); 68% are uncratered (e–d) etc., (see also text).

We will now proceed to the time dependent aspects of the detailed bombardment history of both the surviving and destroyed rocks. Figure 5 presents the history of the entire rock population; details referring to the survivors are also illustrated. The most significant line separates the number of rocks destroyed from those that are still surviving; these are furthermore classified in uncratered and cratered rocks. The uncratered field simply represents that fraction of the surviving rock population that has not suffered at all any event with energies $\geqslant 0.1E_R$. The numbers in the cratered field indicate how many times specific fractions of surviving rocks have been impacted with events of unspecified magnitude, i.e., number of all events $\geqslant 0.1E_R$. At unit time, 50% of the rocks are destroyed; the remaining survivors have, in most part, suffered multiple impacts, e.g., $\approx 10\%$ of the original population has been impacted more than 5 times. As time progresses, e.g., at model time 3.2, all survivors ($=1\%$ of original population) will have suffered 3 impacts. Approximately 0.06%, 0.35% and 1.6% of the original population will experience as many as 9, 8 and 7 cratering events respectively before rupture is accomplished.

The numbers of impacts on the survivors in Figure 5 simply refer to all events $\geqslant 0.1E_R$. However, from the detailed histories of individual rocks it is possible to delineate the actual amount of rupture energy accumulated per any given time (Figure 6). The total number of survivors (e.g., in Figure 5) was normalized to 100%;

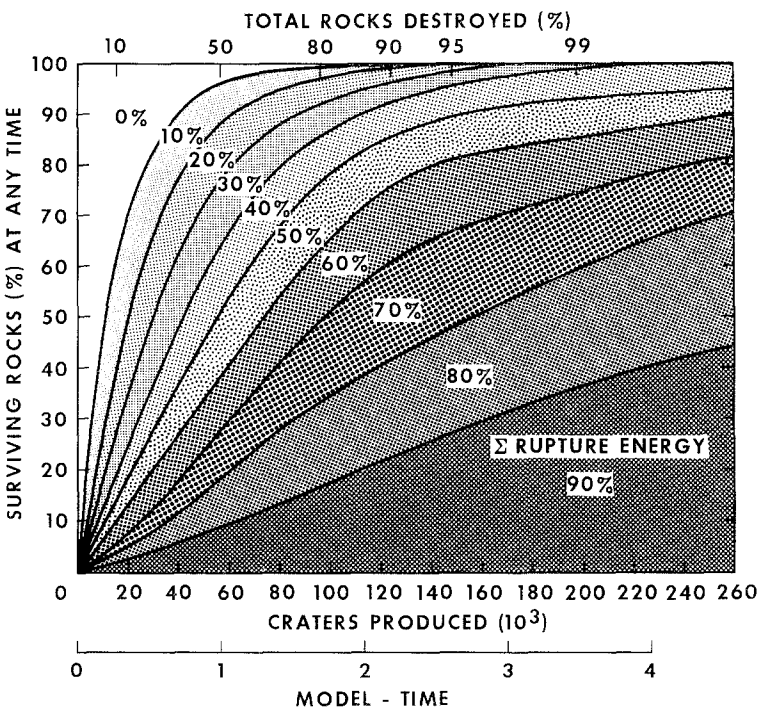

Fig. 6. Accumulation of rupture energy in lunar rocks as a function of time. All percentages are cumulative; differential percentages may be obtained in the fashion described in Figure 5.

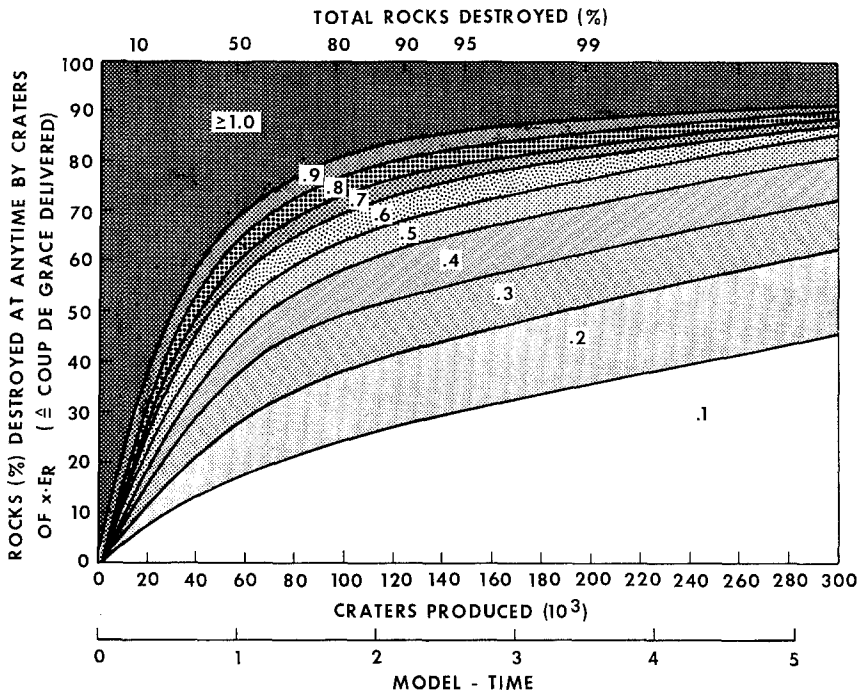

Fig. 7. Magnitude of impact event last contributing to catastrophic rupture, i.e., 'coupe de grace' as a function of time. Rock per cent on y axis are cumulative and refer exclusively to normalized survivors at any particular time; absolute percentage of survivors with respect to original population is the complimentary value of 'total rocks destroyed'. Percentages are cumulative; differential percentages may be obtained similar to Figure 5.

their absolute percentage with respect to the original population may be obtained as the complimentary value to the percentage of rocks destroyed. We see that when 50% of the rocks are destroyed (at model time 1), $\approx 95\%$ of the survivors have accumulated $\geqslant 0.1 E_R$; at the same time, 50% of the survivors have accumulated $\geqslant 50\% E_R$ and more than 10% have accumulated $\geqslant 80\% E_R$. At the 95% destruction level all remaining rocks received at least 20% rupture energy, etc. Because energy is accumulated over time, the destruction of rocks beyond the 50% and especially 90% destruction level is relatively rapid.

The magnitude of the event that actually ruptured the rock (coupe de grace), is shown in Figure 7 with the absolute per cent of survivors again normalized to 100%. It can easily be seen that events $\geqslant 1.0 E_R$ are almost the sole contributors to catastrophic rupture in the early history. As time progresses, smaller and smaller events become more and more effective.

As a consequence the effective contribution of different cratering events during the entire rupture process must vary with time. We therefore determined for individual rocks what magnitude event(s), including the coupe de grace, have contributed to destruction. Some representative results are illustrated in Figure 8 by plotting the

cumulative contributions of various cratering events to the entire rupture process at 4 different model times. Again it can be seen that in the early history events $\geqslant 1.0E_R$ deliver a disproportionally large amount of energy. As time progresses smaller and smaller events will increase in importance. However, only after about model time 3.3 (=99% rocks destroyed) will the individual crater size classes effectively contribute approximately in the manner predicted by the probabilities of Table II.

Summarizing Figures 5–8 it can be concluded that the rupture histories of individual rocks may differ drastically. In the early history rocks are predominantly (if not exclusively) destroyed by the more energetic events; smaller events will be most effective in the late stages, because larger and larger portions of the total rupture energy will then have accumulated in the surviving rocks. Thus the rupture process is accomplished by a complex balance of magnitude and probability of occurrence for specific events. These effects explain also why the differential numbers of rocks destroyed per time interval indicated in Figure 3 are intermediate at the beginning and

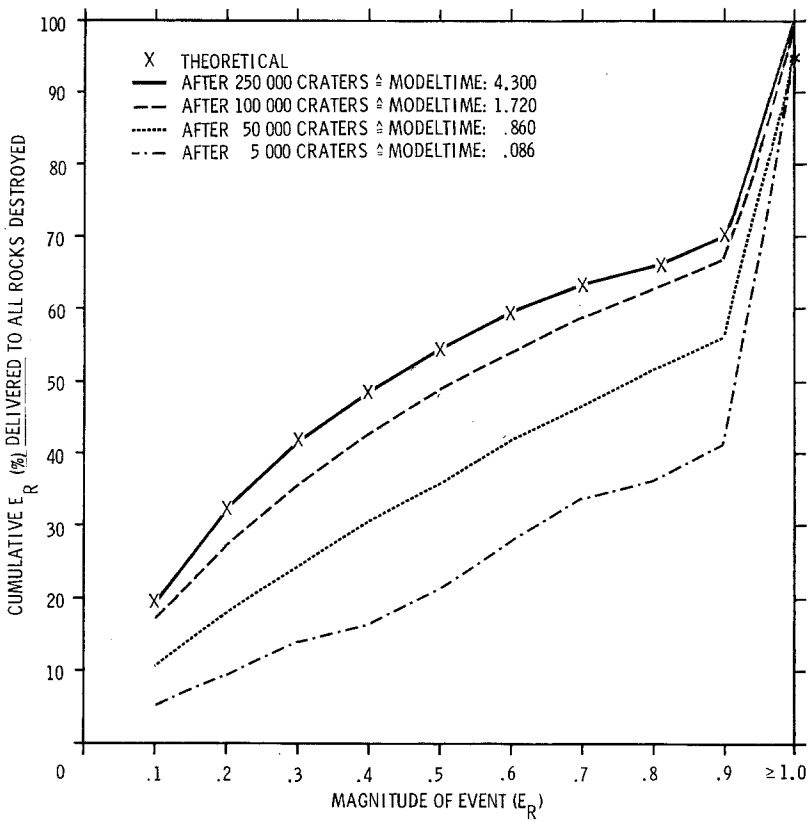

Fig. 8. Relative contributions of impacts of various magnitudes to the actual destruction of lunar rocks at four different model times. The cumulative E_R was obtained from the bombardment history of all rocks destroyed, which are normalized to 100%. Unit time corresponds to the mean survival time and therefore absolute percentages of rocks destroyed may be obtained from previous figures.

why they reach a maximum somewhat later. The gradual accumulation of rupture energy also explains why the destruction of rocks beyond the 50% level is relatively fast compared to the effective destruction of a surface layer (Gault *et al.*, 1974; Hörz *et al.*, 1974). While the model time between the 50% and 99% level of destruction for catastrophic rupture is approximately 5, the corresponding time interval is approximately 7.5 for the destruction of a surface layer.

4. Absolute Rock Masses

The model results refer to a population of rocks that consists entirely of rock-specimen of identical, though unspecified cross-section. In order to apply these data to absolute rock masses, one needs to introduce absolute dimensions for the size of the 'unit-cell'. Such dimensions fix not only the model-cross section and thus the mass of a rock, but according to Figure 2 they also define the critical crater diameter $D_s = 1.0E_R$ and thereby the probability of occurrence for all craters $\geqslant 0.1E_R$ (Equation (6), Table II). Because the crater production population and resulting energy frequency distribution (Equation (6)) is characterized by a constant slope, the occurrence of rupture energies of $1.0E_{R_x}$, $1.0E_{R_y}$ and $1.0E_{R_z}$ destroying masses x, y and z respectively are also defined by Equation (6). As a consequence it is possible to specify relative times for destruction of any absolute rock mass rather precisely.

Figure 9 presents a summary of these calculations for rocks ranging in mass from 10^{-2} to 10^{7} g. Rocks smaller than 10^{-2} g have not been treated in this analysis,

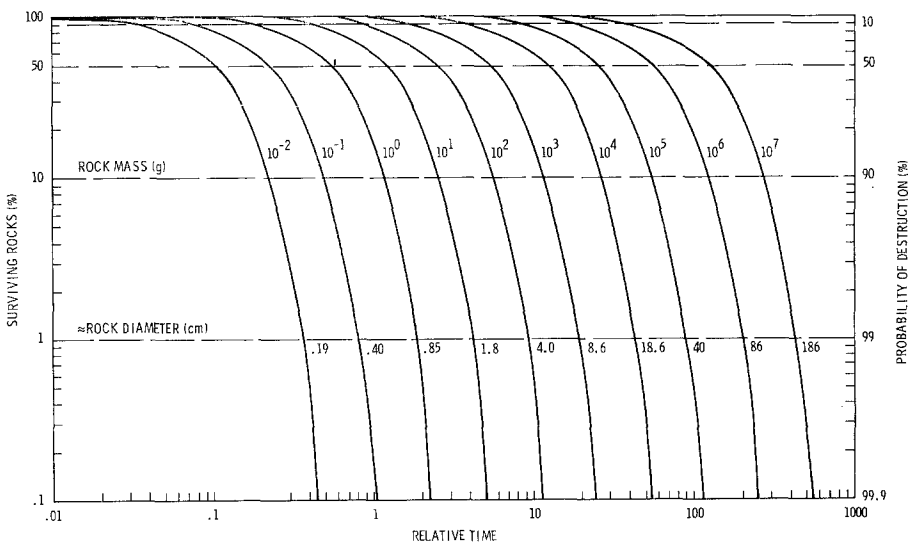

Fig. 9. Relative survival times for various absolute rock masses. Unit time is completely arbitrary. For reasons of clarity, not all curves are drawn through their proper origin in the upper left hand corner (0.01/100%). Notice how efficient relatively small masses are destroyed and – conversely – to what degree populations of large masses may remain essentially unmodified for extremely long periods (see also text).

because their rupture process will be affected by crater-size distributions that differ from Equation (4); rock masses $>10^7$ g were not considered, because of uncertainties in extrapolating (= scaling) the rupture energies to significantly larger masses. The rupture energies are best defined for rocks ranging from 10^2 to 10^4 g.

Referring to Figure 9 it can be seen that 'small' rock masses are destroyed relatively fast, e.g., it takes time 1 to destroy 99.9% of all 0.1 g rocks and it will take about 2.2 times longer to destroy most 1.0 g rocks, etc. Furthermore consider the case when the probability of destruction for 10^3 g rocks reaches 90% at model time 10; within 10 time intervals all rocks of mass 10^2 also generated at time 0 would be destroyed. Because it will take an additional 15 time periods to destroy the remaining 10^3 g specimen (total destruction time is 25), sufficient time remains (i.e., 15 units) to destroy all newly generated fragments $\leqslant 10^2$ g from the first 90% of the 10^3 g population. As a consequence the majority of fragmentation products resulting from the rupture process itself will be thoroughly comminuted prior to the complete destruction of the respective parent population, in particular those fragments that have masse less than 10% of the parent boulder.

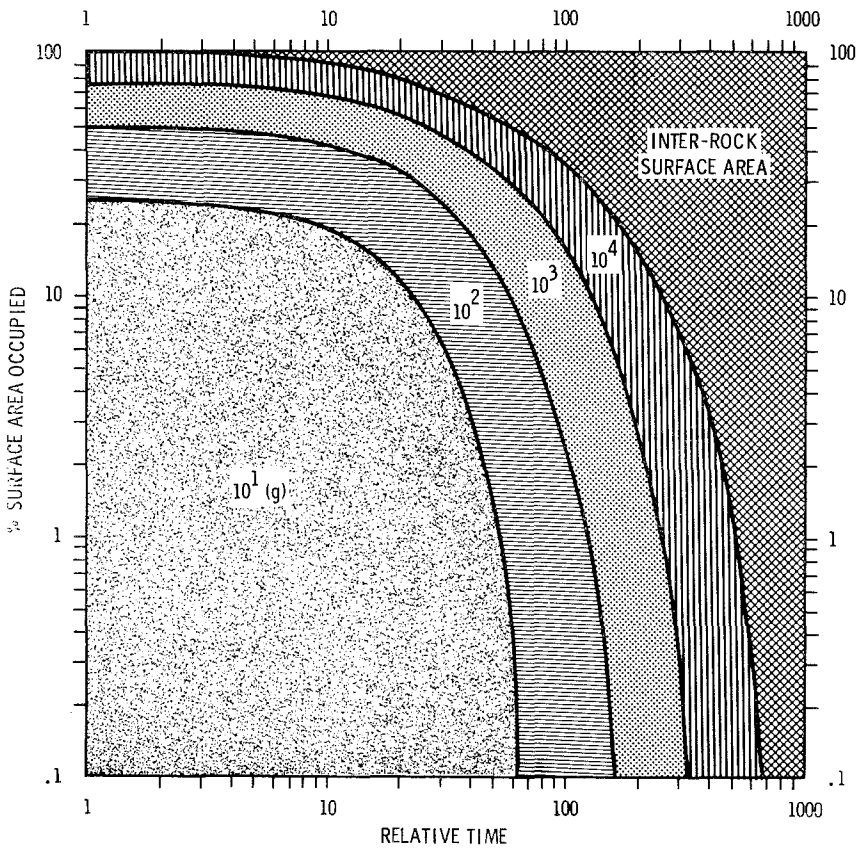

Fig. 10. Evolution of the lunar surface initially covered by four different rock masses, each occupying 25% of the surface. Relative time is completely arbitrary (for details see text).

The relative times indicated in Figure 9 may also be used to reconstruct the history of any hypothetical rock population that is characterized by a variety of rock masses, provided each differential mass does occupy a statistically significant fraction of the surface. An example is given in Figure 10, for rocks of masses 10^1, 10^2, 10^3 and 10^4 g, assuming that they were generated at the same time in such proportions that they cover 25% each of the total surface. Straightforward extrapolation of Figure 9 will then give the history of each mass group. More and more surface area initially occupied by rocks will be destroyed and – conversely – more and more interrock area is generated. Though the absolute surface area occupied by rock specimen decreases, larger rock masses will occupy relatively larger and larger fractions of that area, e.g., at an arbitrary model time 10 the initial conditions (25% each) have changed to 19% (10^1 g), 24% (10^2 g), 24.8% (10^3 g) and essentially 25% (10^4 g). At model time '60' the corresponding values are 0.25% (10^1 g), 8.7% (10^2 g), 17.9% (10^3 g) and 22.2% (10^4 g). Finally at model times >300 the only significant survivors will be rocks of 10^4 g.

It has to be emphasized that Figure 10 and other associated implications are of limited value to the real lunar surface, because only the rupture history of the original population is considered. In reality, however, a lunar rock population is made up of both the original population and its fragmentation products. The latter ones are not considered in Figure 10. They may – especially in the early history – make up a major fraction of the observable rock population. Furthermore lunar rocks in the most general geologic situation are brought to the regolith surface in a continuous fashion, rather than at one instant in time.

However, the latter model assumption may be applicable to the ejecta blanket of impact craters. Knowing the original size distribution of primary ejecta, detailed boulder counting around lunar craters should, in principle, reveal a bimodal mass frequency distribution. The frequency of the largest masses should be close (or closest) to the original distribution, as they are the least affected. An inflection separating the essentially unaffected from affected masses as determined from a 'standard' distribution may yield relative formation ages of various sized lunar craters.

5. Flux-Dependent Implication

In order to convert the model times presented above into absolute lunar surface residence times, the crater size frequency distribution (Equation (4)) must be associated with an absolute crater production rate. Microcrater studies on lunar rocks have lead to an improved understanding of the micrometeoroid environment on the lunar surface averaged over the last few 10^6 yr and resulting crater-production rates for 0.1 to -1 cm diameter impact craters (D_s). Uncertainties within a factor of 5, however, still exist. It is important to note that this MC model employs observable crater production rates, rather than meteoroid mass fluxes. Thus all uncertainties concerning cratering mechanics that may be inherent in converting an observed crater diameter into a projectile mass are eliminated. We strictly employ observed crater-production rates to calculate the absolute number of craters produced and thereby to

solve for absolute times. According to Hartung and Storzer (1974) and Hörz *et al.* (1975) the following crater production rates are representative over the past 10^6 yr for craters with pit diameters $\geqslant 0.05$ cm ($D_s \geqslant 0.2$ cm):

RATE I (MINIMUM)

1.2 craters/10^6 yr cm^{-2} (based on rock 68415, i.e., crater counts by Neukum *et al.* (1973) and surface exposure age by Crozaz *et al.* (1974)).

RATE II (BEST ESTIMATE FOR AVERAGE METEOROID ACTIVITY)

5.0 craters/10^6 yr cm^{-2} according to rocks 12017, 12038, 12054 and 69935 (Hörz *et al.*, 1971; Hartung *et al.*, 1972; Neukum *et al.*, 1973; Fleischer *et al.*, 1971; Bhandari *et al.*, 1972; Schonfeld, 1971; and Crozaz *et al.*, 1974).

RATE III (MAXIMUM)

10 craters/10^6 yr cm^{-2}. Hypothetical upper limit; no crater-production rates of this magnitude were observed.

We consider crater production rate II a best estimate for the meteoroid flux during the past 10^6 yr (see e.g., Hörz *et al.*, 1974), and offer accordingly a plot of absolute times for the destruction of a variety of absolute rock masses of general interest to lunar sample interpretations (Figure 11). Absolute times associated with rates I and III would simply be a factor of about 4.2 longer or a factor of 2 shorter respectively.

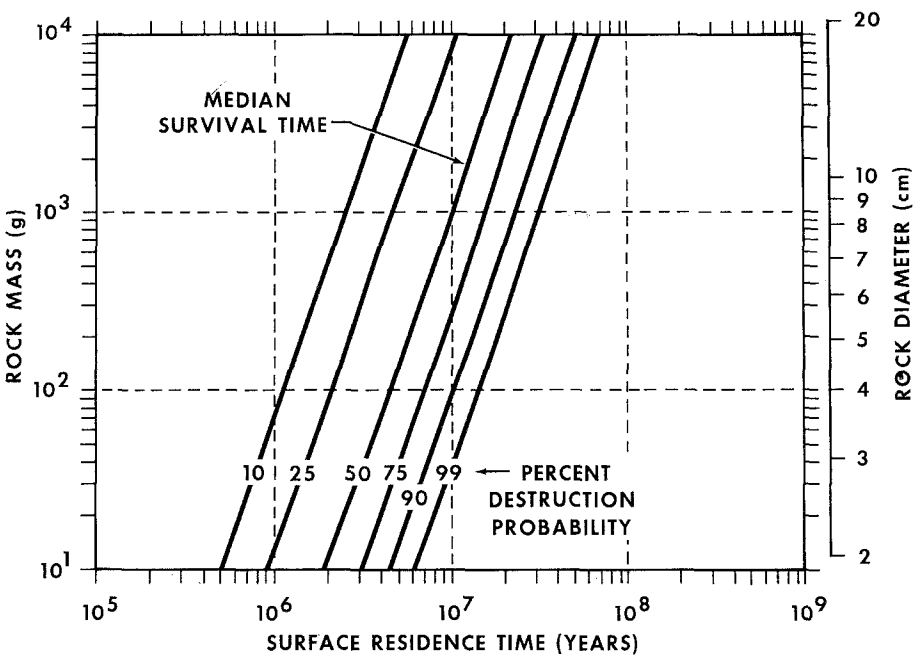

Fig. 11. Absolute times of survival history of various rock masses utilizing a best estimate for the crater production rate of 5 craters $\geqslant 500$ μm pit diam/10^6 yr cm^{-2} (see text).

6. Discussion

Detailed bombardment histories of lunar rocks, until their ultimate catastrophic rupture by meteoroid impact, were studied utilizing MC techniques. The main benefit of such probabilistic approaches is the attainment of the distribution of bombardment histories and the expected lifetimes as opposed to only a mean survival time (e.g., Shoemaker *et al.*, 1971; Gault *et al.*, 1972; and Ashworth and McDonnell, 1973, Table I). Because these previous models do not consider the random nature of the impact process and because they utilize different destruction criteria and/or meteoroid fluxes, we suggest that our new results more adequately describe the history of lunar rocks. The results permit useful insight into the general, time dependent, processes accomplishing catastrophic rupture of lunar rocks. However, it must be emphasized that the absolute time scales proposed are critically dependent on our evolving knowledge of the meteorite environment during the last few tens of million years.

Furthermore the MC model, in part, oversimplifies lunar reality in one significant aspect: all model rock populations are generated at one instant in time. Genuine lunar rock populations, however, are generated at random time intervals and existing rock populations are continuously replenished with freshly excavated materials. Furthermore lunar rock populations are also continuously modified by the addition of fragmentation products of the rupture process itself, leading in reality to an increase in the number of small specimen, rather than a decrease as predicted by our calculations. Rocks are not simply removed form the lunar rock inventory, but are continuously added to the inventory of small and smaller grain-sizes. Accurate size frequency distributions of the fragmentation products are difficult to predict, because Gault and Wedekind (1969) demonstrated qualitatively that fragment size is strongly controlled by the rupture history of the parent rock, i.e., a rock destroyed by the cumulative effects of low energy events will have fewer and larger fragments than a rock destroyed by a single event of exactly $1.0E_R$; these grain size distributions, in turn, will differ from still more fine grained fragments obtained when a rock is ruptured by a single event with energies $\gg 1.0E_R$. As a consequence the comminution of fragmentation products cannot be considered in detail in this MC model. It must, however, be recognized as an important aspect of regolith processes leading from rocks to soil (Shoemaker, 1971).

The general validity of our MC model, however, may be assessed by comparing our survival times with actually measured surface residence times of lunar rocks. Such residence times are based on 3 entirely different techniques: solar and galactic particle tracks, short lived radio active isotopes and cosmogenic or spallation noble gases. Sensitive testing of our predictions is possible only with solar wind and flare dependent parameters, i.e., shortlived radioisotopes and solar flare tracks (SFT), because of their characteristic, shallow penetration production profiles. Other parameters may not necessarily be indicative of true surface exposure. Unfortunately also the shortlived radioisotopes and the SFT cannot distinguish between exposure while

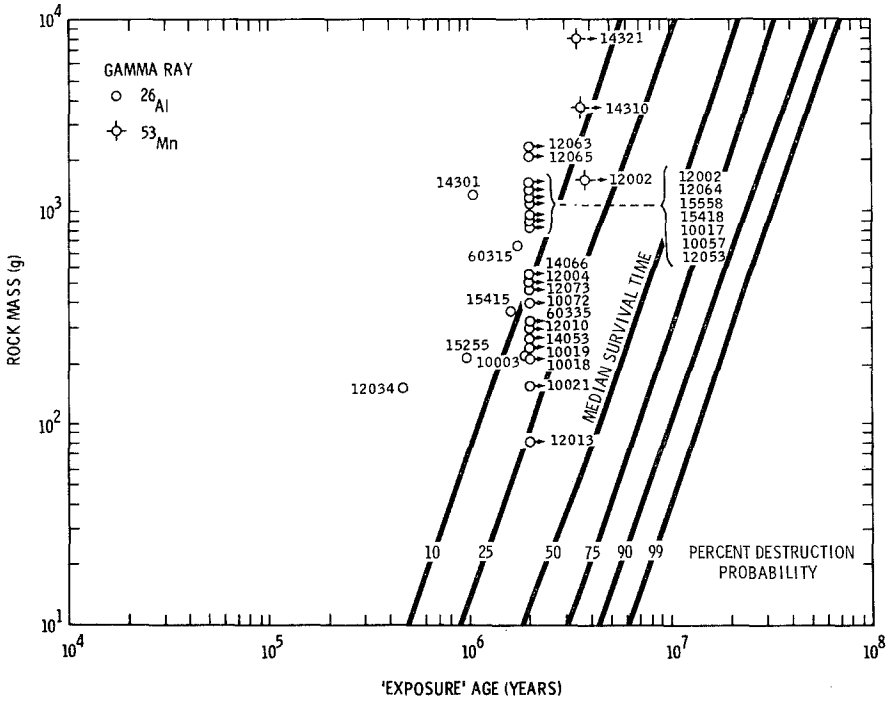

Fig. 12. Comparison of calculated survival times for lunar rocks and surface residence times of specific samples based on short lived radioactive isotopes. Owing to saturation effects, mostly minimum surface residence times may be obtained from such rocks.

the specimen was sitting loosely on the surface (essentially possessing its present shape and mass) or whether part of the exposure occurred on a bigger parent boulder. As a consequence the following comparison cannot be exact, but it constitutes a useful evaluation concerning consistency of a large variety of data.

First consider the most sensitive technique, i.e., shortlived radioisotopes (Figure 12). The exposure data utilized are taken from Keith and Clark, 1973; Wahlen *et al.*, 1972; Imamura *et al.*, 1974). All measurements appear consistent with the MC model because none of the γ-ray exposure ages exceeds the predicted 99% destruction time. However, owing to saturation-effects for shortlived isotopes not very many accurate exposure ages exist. Most of the data quoted represent minimum values, i.e., the rocks must have been exposed to space longer than indicated.

Figure 13 is a similar representation for the track data as tabulated by Crozaz *et al.* (1974). Basically three different sets of data are distinguished, thus simplifying somewhat the original tabulation by Crozaz *et al.* (1974). The most accurate data originate from rocks for which the gradients of both the solar flare tracks (SFT) and galactic tracks (GT) are measured ($\triangleq$ SFT + GT). The 'SFT only' measurements refer to track studies generally confined to the upper mm of a rock and therefore are affected by small-scale exposure geometry, degree of erosion and surface area selected i.e., by a

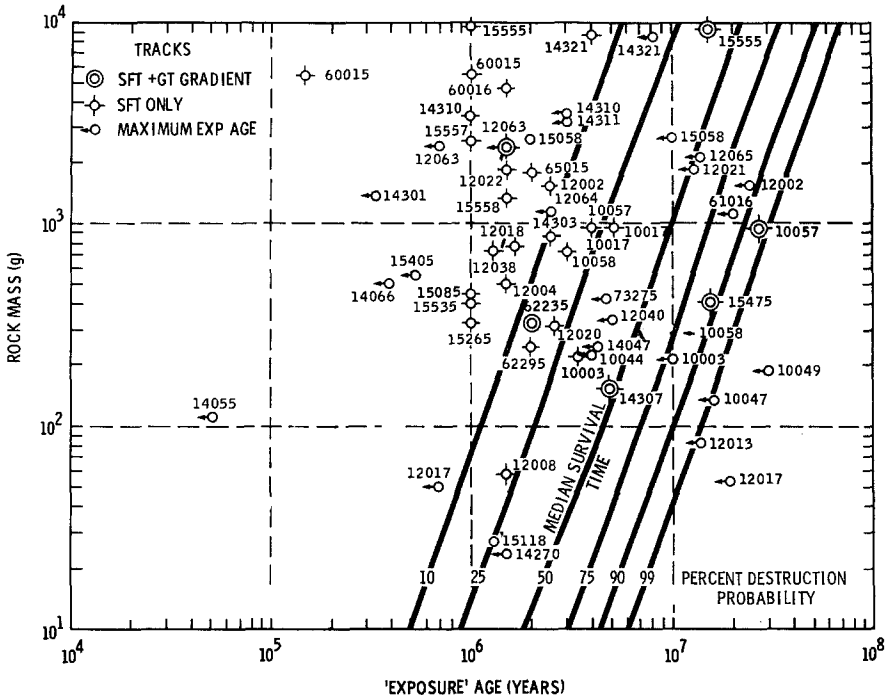

Fig. 13. Comparison of calculated survival times of various rock masses and a variety of absolute exposure ages based on solar flare and galactic particle tracks of specific lunar rocks (see text).

variety of parameters that cannot easily be quantified (e.g., Lal, 1972; Crozaz *et al.*, 1974). Finally the 'maximum exposure' ages are based on track densities inside a rock, most likely at the center. Because of the relatively deep penetration of the GT production profile – as opposed to SFT – these maximum ages can have accumulated under certain, modest shielding conditions and may not reflect genuine exposure at the lunar surface. It is therefore concluded that none of the track exposure ages appear to be inconsistent with our rupture calculations.

Figure 14 presents exposure ages based on noble gases (Bogard *et al.*, 1971; Bogard and Morrison, 1974, (pers. comm.); and Pepin *et al.*, 1974). The vast majority of noble gas exposure ages exceeds significantly the expected surface residence times of this MC model. This is not surprising, because the respective gas production profiles penetrate to depths measured in m (e.g., Pepin *et al.*, 1974). With the notable exception of some Apollo 14 and 16 samples, which clearly are the products of the Cone-, South Ray- and North Ray-cratering events, all rocks returned must have resided within the regolith for periods of tens to hundreds of million years. Rocks can generally not reside on the very lunar surface longer than the times calculated in this MC model. Thus additional exposure to the noble gas production profile(s) must have occurred in the subsurface, i.e., within the regolith (or large parent boulders). We therefore agree

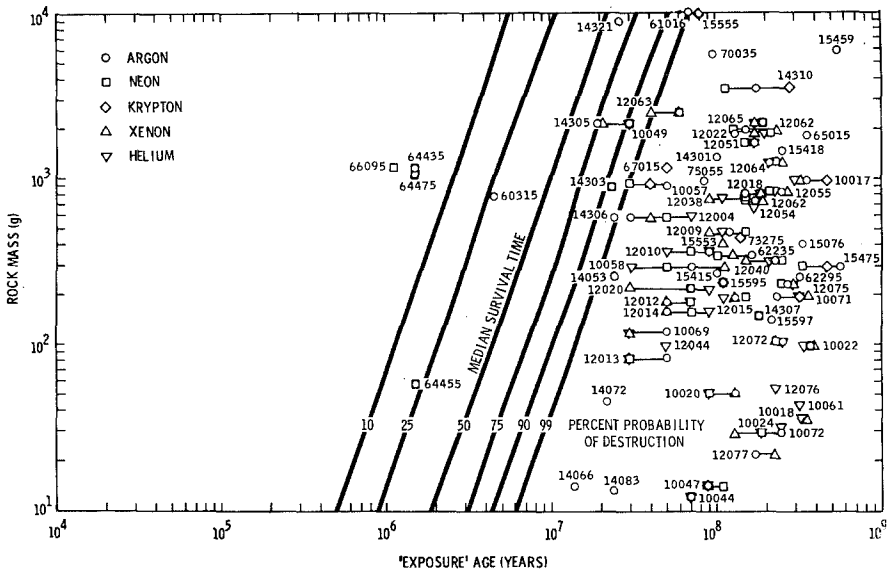

Fig. 14. Comparison of calculated survival times of various rock masses and a variety of noble gas spallation ages for specific lunar rocks (see text).

with previous conclusions that most rocks collected were exhumed from within the regolith, rather than from unirradiated bedrock.

We now compare the catastrophic rupture process with single particle abrasion (see Table I) and determine, which of the two processes dominates the comminution of lunar rocks. Rocks simulated in this MC model were assumed to be of constant cross-section, hence mass, throughout their entire surface residence time; simultaneous particle abrasion was not simulated. Figure 15 illustrates, in a schematic manner, two examples for comparison. Rocks of initially 5 and 10 cm diam were assumed to suffer single particle abrasion rates of 0.5 and 1 mm 10^6 yr^{-1}. At the 50% destruction level ($\approx 11 \times 10^6$ yr), the original 10 cm diam rock has been eroded to 9.45 cm diam, or 8.9 cm respectively, postulating 4π exposure geometry. When the rock reaches the 99% destruction level (36×10^6 yr), it will have an effective diameter of 8.2 or 6.4 cm respectively, depending on the erosion rate assumed. Thus even assuming 1 mm/10^6 yr abrasion, all 'eroded' rocks remain of considerable size before they suffer destruction by rupture. The significant point is that at any given time more total mass will be comminuted by the rupture process than by single particle abrasion, a conclusion also reached earlier by Shoemaker (1971) and Gault *et al.* (1972).

The time Δ in Figure 15 indicates the maximum potential decrease in survival time if one also considers the continuously decreasing effective cross-section caused by single particle abrasion. Consequently maximum survival times indicated in Figures 11–14 could be as much as 25% or 15% shorter than calculated, depending on particle abrasion rates of 1.0 mm or 0.5 mm/10^6 yr, respectively. Such decreased survival

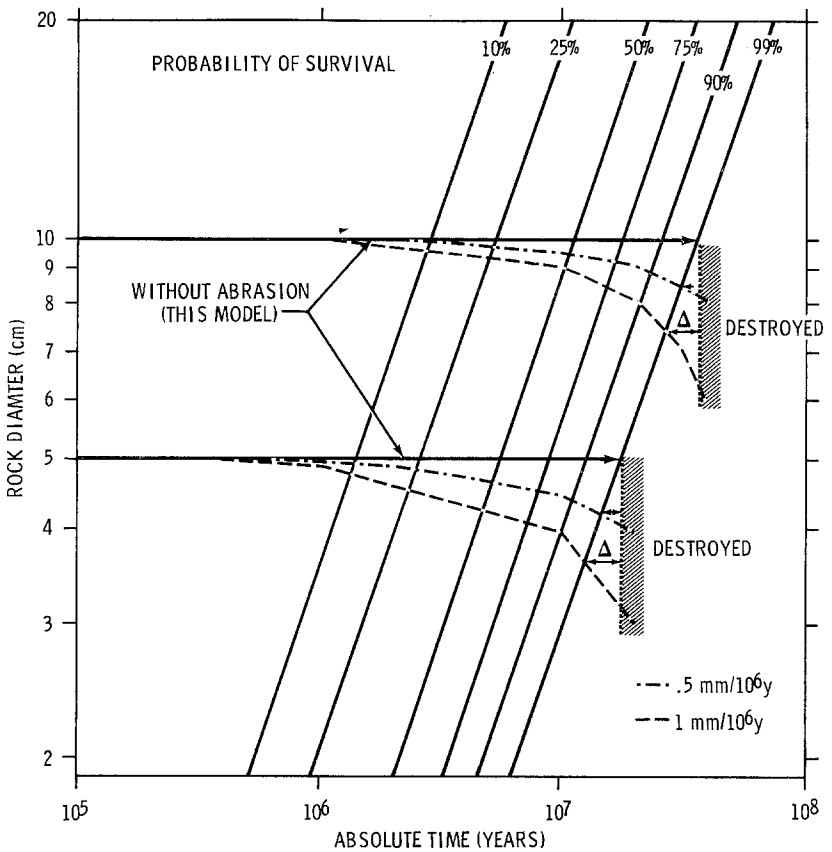

Fig. 15. Comparison of 'single particle abrasion' and 'catastrophic rupture' processes for 2 rocks of 5 and 10 cm respectively diameter subjected to single particle abrasion rates of 0.0, 0.5 and 1 mm 10^6 yr^{-1}. The rocks are considered destroyed beyond the 99% level of destruction.

times should even more enhance the above conclusion, that catastrophic rupture is the primary process for the destruction and comminution of lunar rocks.

Furthermore the effects of the unconfined compressive strength (S_c) of the target need to be discussed. As indicated in Equation (1), rupture energy is a function of target strength. Assuming a constant density for any given rock, the model times calculated will vary according to the ratio $[S_{c\,(x\text{ kb})}/S_{c\,(3\text{ kb})}]^{0.45}$. Since 3 kb is the upper limit for crystalline rocks, most lunar breccias will rupture in shorter times. If in addition to smaller target strength, bulk densities other than 3 g cm^{-3} (the assumed value in this model) are postulated, the rupture times may also vary, i.e., they will decrease for densities <3 g cm^{-3} and will increase for >3 g cm^{-3} (see Equation (3)). Any given set of data may easily be related utilizing Equation (1) and (3) to this model, which is based on 3 kb compressive strength and a bulk density of 3 g cm^{-3}.

7. Conclusions

The rupture history of lunar rock populations was simulated. It was demonstrated that the median survival time is approximately a factor of 5 shorter than the time required to destroy 99% of the rocks. Small rocks are destroyed with great efficiency and it appears likely that relatively large rock masses remain for considerable time periods as the sole survivors of a lunar surface event, e.g., an impact crater ejecta blanket (Shoemaker, 1971). Furthermore the catastrophic rupture dominates mass wasting in the comminution and obliteration of lunar rocks, as already concluded by Shoemaker (1971) and Gault *et al.* (1972). The calculated surface residence times are consistent with presently available information on exposure histories of specific rocks.

Acknowledgements

Helpful comments by V. R. Oberbeck and H. Zook are appreciated. Furthermore, E. S. and J. B. H. gratefully acknowledge partial support by the Lunar Science Institute, Houston, Tex., which is operated by the Universities Space Research Association under Contract No. NSR 09-051-001 with the National Aeronautics and Space Administration.

References

Arnold, J. F.: 1975, this issue, p. 159.
Ashworth, D. G., McDonnell, J. A. M.: 1973, *Space Res.* **XIII**, 1071–1083.
Bhandari, N., Goswami, J. N., Gupta, S. K., Lal, D., Tamhane, A. S., and Venkatavaradan, V. S.: 1972, *Proc. Third Lunar Sci. Conf.*, 2811–2829.
Bogard, D. D., Funkhouser, J. G., Schaeffer, O. A., and Zähringer, J.: 1971, *J. Geophys. Res.* **76**, 2757–2779.
Crozaz, G., Walker, R., and Woolum, D.: 1971, *Proc. Second Lunar Sci. Conf.*, 2543–2558.
Crozaz, G., Drozd, R., Hohenberg, C., Morgan, C., Ralson, C., Walker, R., and Yuhas, D.: 1974, *Proc. Fifth Lunar Sci. Conf.*, 2475–2499.
Dohnanyi, J. S.: 1972, *Icarus* **17**, 1–48.
Fleischer, R. L., Hart, H. R., Comstock, G. M., and Evwaraye, A. O.: 1971, *Proc. Second Lunar Sci. Conf.*, 2559–2568.
Gault, D. E.: 1969, *Trans. Am. Geophys. Union* **50**, 219
Gault, D. E.: 1973, *The Moon* **6**, 32–44.
Gault, D. E. and Wedekind, J. A.: 1969, *J. Geophys. Res.* **74**, 6780–6794.
Gault, D. E., Hörz, F., and Hartung, J. B.: 1972, *Proc. Third Lunar Sci. Conf.*, 2713–2734.
Gault, D. E., Hörz, F., Brownlee, D. E., and Hartung, J. B.: 1974, *Proc. Fifth Lunar Sci. Conf.*, 2365–2386.
Hartung, J. B. and Storzer, D.: 1974, *Proc. Fifth Lunar Sci. Conf.*, 2527–2541.
Hartung, J. B., Hörz, F., and Gault, D. E.: 1972, *Proc. Fourth Lunar Sci. Conf.*, 2735–2753.
Hartung, J. B., Hörz, F., Aitken, F. K., Gault, D. E., Brownlee, D. E.: 1973, *Proc. Fourth Lunar Sci. Conf.*, 3213–3234.
Hörz, F., Hartung, J. B., and Gault, D. E.: 1971, *J. Geophys. Res.* **76**, 5770–5798.
Hörz, F., Schneider, E., and Hill, R. E.: 1974, *Proc. Fifth Lunar Sci. Conf.*, 2397–2412.
Hörz, F., Brownlee, D. E., Fechtig, H., Hartung, J. B., Morrison, D. A., Neukum, G., Schneider, E., and Vedder, J. F.: 1975, *Planetary Space Sci.* **23**, 151–172.
Imamura, M., Nishizumi, K., Honda, M., Finkel, R. C., Arnold, J. R., and Kohl, C. P.: 1974, *Proc. Fifth Lunar Sci. Conf.*, 2093–2103.
Keith, J. E. and Clark, R. S.: 1974, *Proc. Fifth Lunar Sci. Conf.*, 2105–2119.

Lal, D.: 1972, *Space Sci. Rev.* **14**, 3–102.
Latham, G., Dorman, J., Duennebier, F., Ewing, M., Lammlein, D., and Nakamura, Y.: 1973, *Proc. Fourth Lunar Sci. Conf.*, 2515–2527.
Morrison, D. A., McKay, D. S., Heiken, G. H., and Moore, H. J.: 1972, *Proc. Third Lunar Sci. Conf.*, 2767–2791.
Neukum, G.: 1973, *Lunar Science IV*, Abstracts, p. 558–560, Lunar Sci. Inst., Houston, Tex., U.S.A.
Neukum, G., Hörz, F., Morrison, D. A., and Hartung, J. B.: 1973, *Proc. Fourth Lunar* Sci. Conf., 3255–3276.
Pepin, R. O., Basford, J. R., Dragon, J. C., Coscio, M. R., and Murthy, V. R.: 1974, *Proc. Fifth Lunar Sci. Conf.*, 2149–2184.
Quaide, W. L. and Oberbeck, V. R.: 1975, this issue, p. 27.
Schneider, E. and Hörz, F.: 1974, *Icarus* **22**, 459–473.
Schonfeld, E.: 1971, personal communication.
Shoemaker, E. M.: 1971, *Inst. Invest. Geol.* **XXV**, 27–56, Universidad de Barcelona.
Shoemaker, E. M., Hait, M. H., Swann, G. A., Schleicher, D. L., Schaber, G. G., Sutton, R. L., Dahlem, D. H., Goddard, E. N., and Waters, A. C.: 1970, *Proc. Apollo 11 Lunar Sci. Conf.*, 2399–2412.